L3

X-RAY LABORATORY WITH ROTATING ANODE OF THE CONSORTIUM MULTIDISC OF SAS – CAPABILITIES OF THE DIFFRACTOMETER BRUKER D8 DISCOVER SSS

E. Dobročka[1], M. Jergel[2]

[1]*Institute of Electrical Engineering, SAS, Dúbravská cesta 9, 841 04, Bratislava, Slovakia*
[2]*Institute of Physics, SAS, Dúbravská cesta 9, 845 11, Bratislava, Slovakia*
elekdobr@savba.sk

A brief history of an X-ray laboratory of Consortium MULTIDISC founded by several institutes of the Slovak Academy of Sciences is outlined. The diffractometer Bruker D8 DISCOVER with rotating anode located in the laboratory is described. A selection of representative results is introduced to show a wide scope of applications of the diffractometer covering different types of structural analyses.

Introduction

The history of our X-ray laboratory with rotating anode started in 2005 when the Consortium for multidisciplinary research of materials MULTIDISC was established. At present, four institutes of the Slovak Academy of Sciences – Institute of Physics (IP), Institute of Electrical Engineering (IEE), Institute of Inorganic Chemistry (IACH) and Institute of Materials & Machine Mechanics (IMMM) participate in the Consortium with full membership. One institute – Institute of Measurements (IM) is joined as an associated member. The first activity of the Consortium was to establish an X-ray laboratory equipped with a high power X-ray source suitable for thin film analyses. It was concluded that an X-ray tube with rotating anode is the solution that meets the most of the requirements of the Consortium members. The diffractometer Bruker D8 DISCOVER SSS was delivered in December 2005, being the first X-ray generator with rotating anode installed in Slovakia. It was commissioned in February 2006. The new X-ray laboratory is located at the IM of SAS.

Instrumentation

The X-ray tube with rotating Cu anode (line focus 10 x 0.5 mm) is designed for the maximum power of 18 kW, but in practice 12 kW is used for all measurements. The Göbel mirror attached to the body of the tube delivers a quasi-parallel primary beam 1.2 mm wide and with a divergence of ~ 0.03 . This solution is suited for thin film analyses but excludes the possibility to change the set-up to Bragg-Brentano geometry. The automatic absorber (4 values of absorption factor) enables to measure the intensities over 9 orders of magnitude. The central Eulerian cradle allows to perform texture and stress analysis. A precise sample alignment is supported by motorized sample stage (X, Y in-plane shifts by +/- 40 mm, Z shift ranges from -1 to +2 mm). The radiation is collected by a NaI(Tl) scintillation point detector. The diffractometer design is modular with a 4-bounce Bartels monochromator for the primary beam with two Ge(022) channel-cut crystals, a pathfinder for the diffracted beam switching automatically between a slit and a 3-bounce Ge(022) channel-cut crystal analyzer, two Soller slits (0.12 and 0.35 divergence) for coplanar grazing incidence diffraction, a LiF monochromator for suppression of sample fluorescence and a knife-edge collimator for reflectivity measurements. Polycrystalline diffraction in symmetrical (SymD) and grazing incidence (GID) geometries, high-resolution diffraction (HRD), stress, texture and (non-)specular reflectivity (XRR) measurements with evaluation software packages from Bruker are available.

Operation and exploitation of the laboratory

The operating staff of the laboratory has only two members, E. Dobročka (IEE SAS) and M. Jergel (IP SAS). The work for the other two institutes of the Consortium is performed by E. Dobročka.

As mentioned above, the primary task of the laboratory is analyses of thin films prepared by various deposition technologies. This requirement affected considerably the basic set-up and the selection of the optical elements of the diffractometer. As a consequence, Bragg-Brentano geometry is impossible due to the fixed Göbel mirror, aggravating thus investigations of bulk polycrystalline materials. This can be seen in Table 1 where the operating hours-per-year of the diffractometer are shown for all four institutes. Two institutes clearly dominate in the exploitation of the diffractometer which is in agreement with their research field focused on thin film technologies. Nevertheless, the high power of the X-ray tube partly mitigates absence of the benefits of Bragg-Brentano geometry for polycrystalline samples and renders the diffractometer very useful also for IACH and IMMM. A division across particular Departments of the main methods used is the following:

Department of Multilayers and Nanostructures (IP): XRR, diffuse scattering, GID.
Department of Metal Physics (IP): SymD, GID, stress.
Department of Thin Oxide Films (IEE): XRR, GID, HRD.
Department of Optoelectronics (IEE): HRD, texture.
Department of Cryoelectronics (IEE): texture.
Department of Superconductor Physics (IEE): SymD, GID.
Department of Semiconductor Technology and Diagnostics (IEE): GID, HRD.
Department of Ceramics (IACH): SymD, GID.
Department of Hydrosilicates (IACH): SymD.
Department of Properties of Materials & Structures (IMMM): SymD, GID.

Table 1. Exploitation of the diffractometer Bruker D8 DISCOVER SSS during the period 2006-2009. In the columns "hours", the measurement times utilized by individual institutes are given. The columns "%" show the fractions of the total number of hours per year for individual institutes.

	2006		2007		2008		2009	
Institute	hours	%	hours	%	hours	%	hours	%
IP	849	59	293	23	1101	57	738	44
IEE	542	38	831	64	451	23	639	38
IACH	20	1	71	6	160	8	130	8
IMMM	31	2	91	7	220	12	167	10
Total in year	1442	100	1286	100	1932	100	1674	100

Department of Microstructure of Surfaces & Interfaces (IMMM): SymD, GID.

Examples of results

The list of Departments using the services of our X-ray laboratory proves that its research scope is wide. During the whole operation period of the diffractometer, a vast number of results from various scientific fields was obtained. In the following we present just a few examples of measurements that we consider to be either interesting due to surprising results or illustrative to show the capabilities and flexibility of the diffractometer. A comprehensive analysis and interpretation of the results is out of the scope of this contribution and was (or will be) published elsewhere.

Texture analysis of YBaCuO superconductor films grown on GaN

Active and passive elements based on III-V and III-N semiconducting materials are very efficient at the liquid nitrogen temperature which gives a possibility of the integration of passive high-temperature superconductor (HTS) devices with active GaAs and GaN devices in the form of milimeter-wave devices. A direct growth of the HTS thin films on the GaAs, however, can cause damage to the GaAs substrate. This is the reason to examine the possibilities of the YBaCuO deposition on the hexagonal GaN substrate.

The YBaCuO HTS thin films on c-oriented GaN/sapphire substrates were grown at the Department of Cryoelectronics of IEE [1]. Two kinds of samples were prepared. In the first set the YBaCuO film was grown directly on the GaN/sapphire substrate. In the second set a [111]-oriented MgO buffer layer was inserted between the GaN/sapphire substrate and the YBaCuO film as a diffusion barrier.

The texture of both types of samples was analyzed in our X-ray laboratory. The aim of the analysis was to determine the degree of preferred orientation of the YBaCuO blocks with respect to the sample surface normal and to find a possible effect of the MgO buffer layer on the struc-

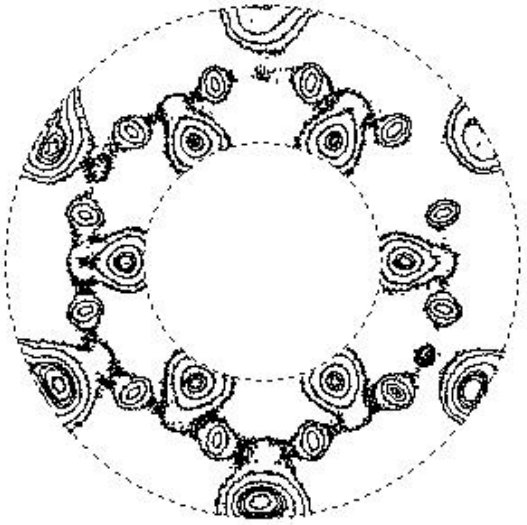

Figure 2. Pole figure (103) of YBaCuO layer grown directly on GaN/sapphire substrate. The range of angle is 30 – 60°.

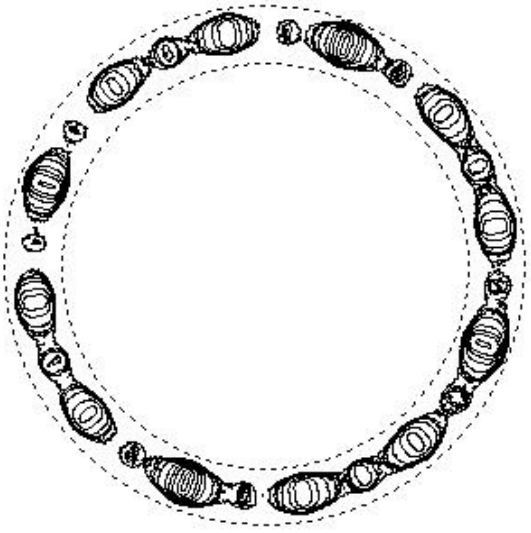

Figure 3. Pole figure (103) of YBaCuO layer grown on MgO buffer layer deposited on GaN/sapphire substrate. The range of angle is 40 – 50°.

tural quality of the HTS films. In Figs. 1 and 2, the (103) pole figures of YBaCuO films grown without and with the MgO buffer layer, respectively, are compared. For the sake of simplicity, here we do not distinguish between the (103) and (013) planes of the orthorhombic YBaCuO lattice due to their similar interplanar distances. The angle between these planes and the c-axis of the YBaCuO lattice is ~45°.¨

In both figures 12 strong and 12 weak maxima can be recognized. While in the sample with MgO buffer layer all maxima are localized around the angle ~45°, in the sample without buffer layer the strongest maxima are at wrong positions indicating that the most of the crystallites have their c-axis inclined with respect to the substrate normal. The in-plane symmetry of both pole figures reflects the combined three-fold symmetry of the (001) GaN or (111) MgO surface and the four-fold one (considering the YBaCuO lattice to be almost tetragonal) of the YBaCuO crystallites. We can conclude that the MgO buffer layer improves the structural quality as well as the superconducting properties of the HTS films grown on GaN/sapphire substrates.

Precipitation of MnAs in InAs epitaxial films

The incorporation of manganese in InAs semiconductor can provide a spintronic material. If the content of Mn exceeds a certain value, precipitation of MnAs phase within the InAs epitaxial layer occurs. As the MnAs particles are hexagonal, interesting orientation relationship between the MnAs lattice and the cubic matrix can be expected. It is assumed that the c-axis of MnAs lattice is perpendicular to the {111} planes of the InAs matrix. However, the diffraction (102) of MnAs is usually visible in the standard 2 / diffraction patterns indicating that precipitates of different orientations are also present in the InAs layer.

The Mn-doped InAs epitaxial layers grown on (001) GaAs substrates were prepared at the Department of Optoelectronics of IEE [2]. We have analyzed a series of samples with various content of Mn but we have found

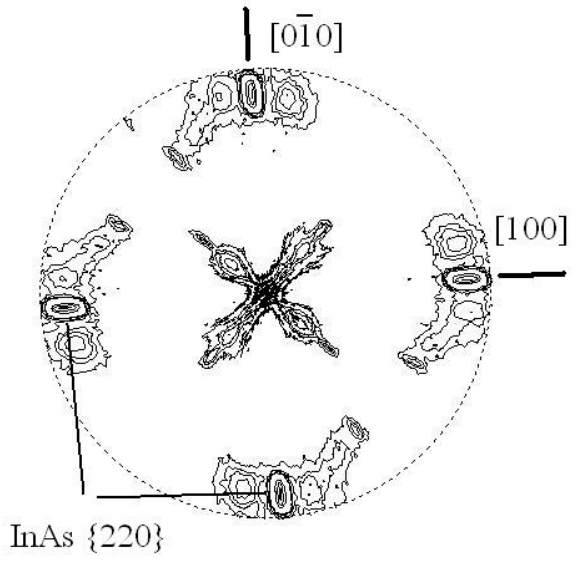

Figure 4. Pole figure (102) of MnAs precipitates in In(Mn)As epitaxial layer. The range of angle is 0 – 50°.

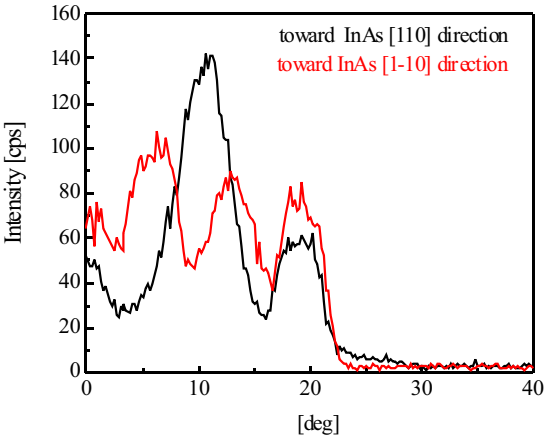

Figure 5. scans of MnAs (102) diffraction toward two perpendicular directions [110] and [1-10] of the InAs layer lattice.

only quantitative differences concerning the orientation distribution of the MnAs precipitates. A typical pole figure (102) of MnAs precipitates is shown in Fig. 5. The strong maxima at the periphery (= 45°) of the figure are caused by the {220} planes of the InAs lattice that have nearly the same interplanar distance as the planes {102} of MnAs. Surprisingly, the figure does not have the expected four-fold symmetry. The c-axes of MnAs precipitates are strongly confined to the (110) and (1-10) planes of the InAs lattice, but their orientation distribution within these planes is different. This difference is even more visible in Fig. 5, where the (102) MnAs scans toward the [110] and [1-10] directions of the InAs matrix are compared. The revealed asymmetry of the orientation distribution of MnAs particles is a direct consequence of the polarity of zinc-blende structure and is probably affected by the mechanism of the epitaxial growth of III-V compound semiconductors.

Spatially resolved diffraction

In the past years a number of studies have been published on various aspects of the reactions between Sn-Ag, Sn-Cu and Sn-Ag-Cu alloys and various substrates. Reaction between Sn in these molten solders and Cu substrate at the Cu/solder interface results in the formation of Cu_6Sn_5 and Cu_3Sn phases. At the Department of Microstructure of Surfaces & Interfaces of IMMM the influence of indium addition to SnAgCu solder on the microstructure of the interface between solder and cupper substrate was studied [3]. Our X-ray laboratory was involved in this analysis with the aim to reveal the spatial distribution of the phases with respect to the solder/Cu interface.

In order to solve this problem, a modification of the grazing incidence set-up was employed. The fixed incidence angle ensured that the width of the irradiated area and the penetration depth did not vary during the measurement and the analysis of the results was simplified. However in contrast to conventional GID, the angle of incidence has been set to 20°. The primary beam was limited by slits to 0.1 x 6 mm size, hence the width of the irradiated area was sufficiently narrow (~0.3 mm) providing a good spatial resolution. The solder/Cu interface was care-

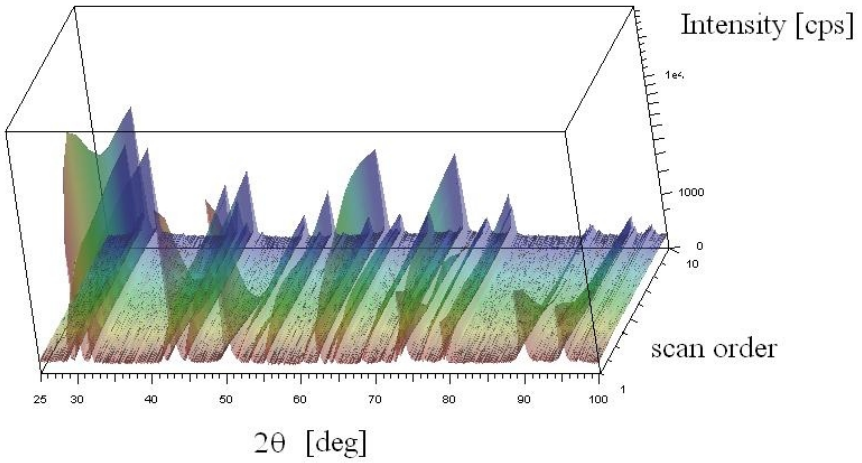

Figure 6. 3D view of a set of detector scans recorded at 10 different positions across the SnAgCuIn solder/Cu interface. Graphical output of the evaluation software EVA (Bruker).

fully adjusted to be parallel to the goniometer axis. At these conditions, a series of detector scans in the range 25 - 100° was recorded at 10 different positions across the interface. The translation parallel to the sample surface and perpendicular to the interface ranged from -0.3 (in Cu substrate) to 1.05 mm with a step of 0.15 mm. In order to maximize the detected intensity, the Soller slit usually used for GID measurements was not inserted into the diffracted beam. The good angular resolution was preserved owing to the small width of the diffracted beam. The variation of diffracted intensities across the interface is shown in Fig. 6 where all ten detector scans are visualized in a 3D view. The first scan corresponds to the position of -0.3 mm. The detailed analysis has been done by inspection of individual scans.

Testing of V-shaped GeSi monochromators

In standard (220) X-ray beam compressing monochromators for Cu K radiation, a total beam compression up to the factor of 10 can be achieved by V-shaped monochromators prepared from a pure germanium single crystal. A higher factor of compression is possible using larger angles of asymmetry. However, the total intensity of the beam is considerably decreased due to the refraction effect. One possibility to overcome this drawback is to use graded GeSi single crystal instead of a pure one.

At the Department of Semiconductor Technology and Diagnostics of IEE V-channel X-ray monochromator with asymmetry factor of 21 was prepared using a linearly graded GeSi single crystal. Rocking curves of the monochromator were measured in our X-ray laboratory in standard and HRD set-ups. The results were compared with those obtained from the reference (pure Ge) monochromator having the same design, as well as from the symmetrical channel cut Ge (220) monochromator. The set-up of HRD measurement is shown in Fig. 7. The width and the height of the primary beam was limited by 0.05 mm and 2.0 mm slits.

On the basis of our measurements we concluded that the intensity loss due to the refraction effect, that takes place in the case of V-channel monochromators, can be compensated by the composition grading of the parent single crystal of the monochromator. In the case of graded

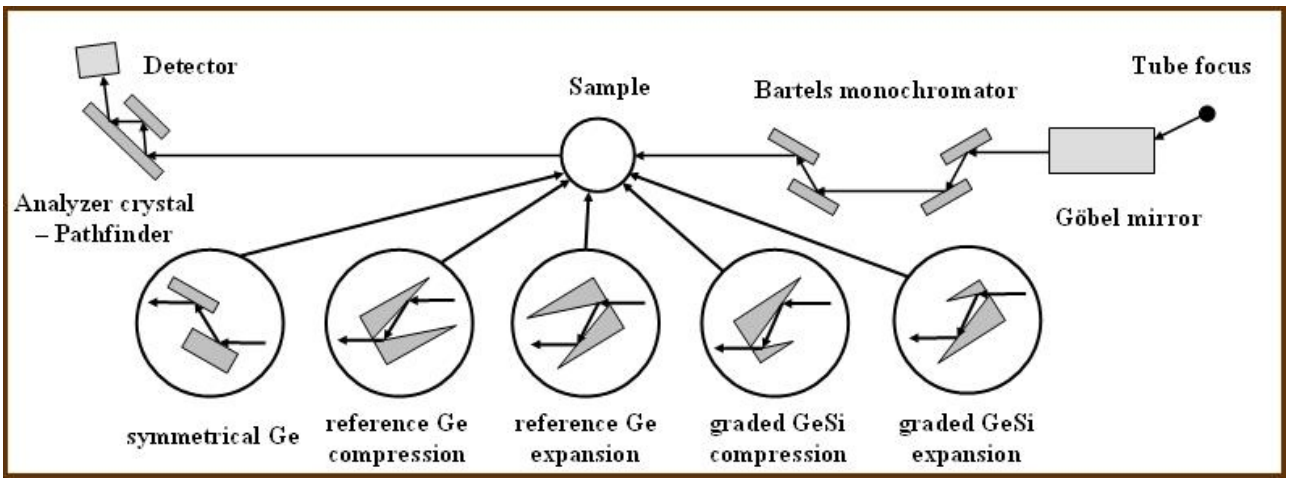

Figure 7. Scheme of the high-resolution set-up. In the circles in lower part of the figure, the top views of the samples and the beam traces are shown for 5 different types of measurement.

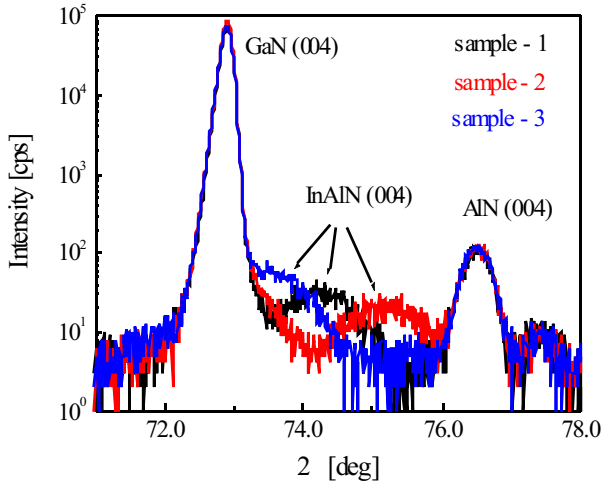

Figure 8. Symmetrical 2 scans of GaN (004) diffraction for three samples with different In content.

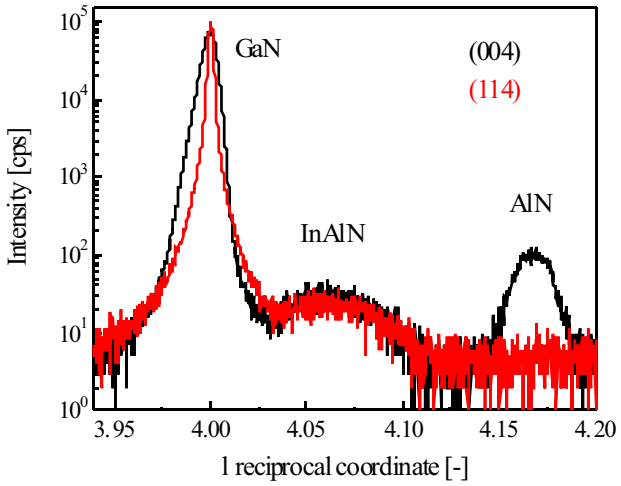

Figure 10. Linear l scans through (004) and (114) points of GaN reciprocal lattice.

GeSi monochromator with the asymmetry factor of 21, more than three times higher intensity was obtained in comparison with the reference monochromator having the same design [4].

HRD – linear scans in reciprocal space

The PC control of the up to date diffractometers enables to perform linear scans in reciprocal space that can be useful for the analysis of lattice mismatch of epitaxial films. For high quality semiconductor compounds the lattice mismatch is of the order of 0.1 % or less and the asymmetric diffractions can easily be measured by standard angular scans. However, in some advanced technologies epitaxial layers with lattice mismatch exceeding 1 % are often used. In this case, the layer diffractions are too far from the substrate ones and the angular scans are inapplicable for measuring the asymmetric diffractions. Instead of performing a complete map of an area in the reciprocal space, linear scans can be used to find the layer peaks.

At the Department of Thin Oxide Films of IEE, InAlN/GaN/AlN/sapphire heterostructures are studied [5]. This system can serve as a good example for demonstrating the advantage of linear scans. In Figs. 8 and 9 2 scans of symmetrical (004) and two asymmetrical (114) diffractions

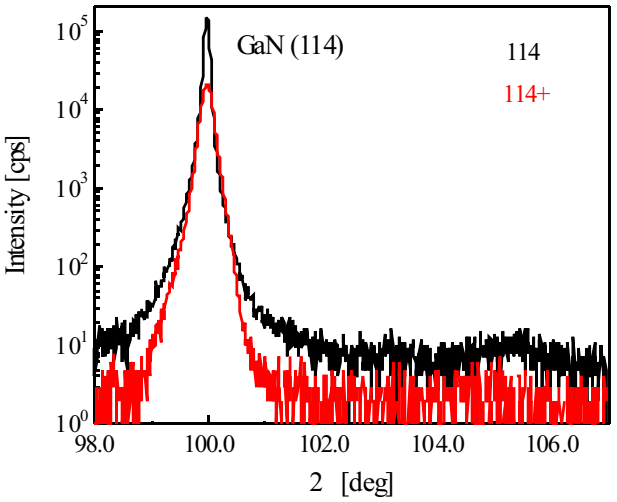

Figure 9. Asymmetrical 2 scans of GaN (114) diffractions of sample – 2. 114– is grazing incidence geometry, 114+ is grazing exit geometry.

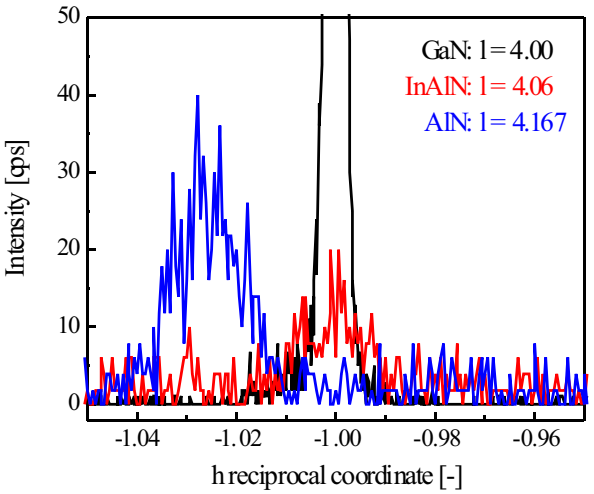

Figure 10. Linear h scans for three different values of l coordinate at the (114) point of GaN reciprocal lattice.

are shown, respectively. The lattice mismatch between InAlN, AlN and GaN is rather large and the peaks of InAlN and AlN layers are missed in asymmetrical scans. However, their position can be determined by linear scans as shown in Figs. 9 and 10.

Firstly, the l coordinate of the layer peaks are read-out from the l scan across the (004) point (Fig. 9). The h scans performed with these values of the l coordinate at the asymmetrical point (114) revealed a perfect lateral match between GaN and InAlN and the shift of the AlN peak by 2.5 % with respect to GaN. All curves except for the h scan at l = 4.00 (Fig. 10) were measured without the analyzer crystal.

Acknowledgement

The work described was supported by SAV-FM-EHP-2008-01-01 project financed within EEA mechanism and MNT-ERA-Net 2007-009-SK project. The support of Slovak Grant Agency for Science (VEGA 2/0031/08) and of Research and Development Support Agency (APVV-LPP-0078-08, APVV-51-0459-06) is also acknowledged.